Pyrolysis of purun tikus (Eleocharis dulcis): Product distributions and reaction kinetics

by Apip Amrullah

Submission date: 25-May-2022 04:50AM (UTC-0400)
Submission ID: 1843824822
File name: Apip_Bid_B_A-10.pdf (2.28M)
Word count: 5134
Character count: 26389

Bioresource Technology Reports 13 (2021) 100642

Contents lists available at ScienceDirect

Bioresource Technology Reports

journal homepage: www.sciencedirect.com/journal/bioresource-technology-reports

Pyrolysis of purun tikus (*Eleocharis dulcis*): Product distributions and reaction kinetics

Apip Amrullah [a,b,*], Obie Farobie [c,d], Rahmat Widyanto [a]

[a] Department of Mechanical Engineering, Lambung Mangkurat University, Banjarmasin, South Kalimantan, Indonesia
[b] Division for Biomass and Energy, Wetland-Based Material (WBM) Research Center, Lambung Mangkurat University, Banjarmasin, South Kalimantan, Indonesia
[c] Department of Mechanical and Biosystem Engineering, Faculty of Agricultural Engineering and Technology, IPB University (Bogor Agricultural University), IPB Darmaga Campus, PO BOX 220, Bogor, West Java 16680, Indonesia
[d] Surfactant and Bioenergy Research Center (SBRC), IPB University (Bogor Agricultural University), Jl. Pajajaran No. 1, IPB Baranangsiang Campus, Bogor, West Java 16144, Indonesia

ARTICLE INFO

Keywords:
Wetland biomass
Purun tikus
Pyrolysis
Phenol
Particle size

ABSTRACT

Pyrolysis of typical wetland biomass, namely purun tikus (*Eleocharis dulcis*) was experimentally studied herein for the first time. The pyrolysis of purun tikus leaves for bio-oil production was conducted under different reaction temperatures (300, 400, and 500 °C) at fixed pressure and different particle size distributions (0.2, 0.4, and 0.6 mm). Characteristics of bio-oil and product distributions were studied. The bio-oil yield as high as 31% was obtained at 500 °C and 0.6 mm of particle size. Meanwhile, the highest bio-char yield of 62% was obtained at 300 °C and 0.2 mm of particle size. The bio-oil was characterized by gas chromatography/mass spectrometry (GC/MS). Phenol yield as high as 18.23% was achieved at 500 °C and 0.6 mm of particle size under atmospheric pressure. A reaction model was proposed, and the reaction kinetic parameters by assuming the first-order kinetics were determined. The reaction was observed to follow the Arrhenius behavior, and the kinetic model agreed well with the experimental data.

1. Introduction

The problems of energy consumption and environmental pollution have motivated researchers to improve and develop technologies and innovations in the renewable energy sector, especially those that can be substituted for fossil fuel resources. Over the past few decades, researchers have sought to explore potential alternative energy sources from renewable energy sources, such as solar, wind, wave, geothermal, and biomass to replace fossil fuels. Among the renewable energy sources which are not competing with food, biomass or its wastes is a strong candidate as an energy source since it is a low cost, abundantly available, sustainable, and able to reduce the greenhouse effect significantly (Abdeshahian et al., 2010; Mortensen et al., 2011).

Biomass, called lignocellulosic biomass, is organic material derived from a living being, such as plants or plant-based products that are not used for food or feed (Paksung and Matsumura, 2015) As a great agricultural and forestry country covered with swamp area, Indonesia can produce a considerable amount of agricultural wastes, forestry residues, as well as tidal swamp plants, which are categorized as wet biomass. Thus, the utilization of biomass is a good option to replace fossil fuel resources in Indonesia for the production of energy and high-value chemicals. Lignocellulosic biomass is mostly composed of a natural polymer, namely cellulose (32–45%), hemicellulose (19–25%), and lignin (14–26%) (Rony et al., 2019). Hence, it can be converted to gaseous, solid, and liquid fuels for the production of heat and power as well as biofuel. In comparison to conventional fossil fuels, the use of biomass energy has many benefits in terms of the shorter life cycles, broader distribution, and lower emissions of greenhouse gases (Cheng et al., 2019).

Several technologies have been employed for biomass conversion to energy, such as thermochemical conversion, biochemical conversion, and physicochemical conversion technology. Thermochemical conversion is the most popular technology to convert biomass due to the fact that it is fast and no limitations for processing mixtures of various kinds of biomass (Dhyani and Bhaskar, 2018). The thermochemical process can be conducted by combustion, torrefaction, gasification (Amrullah and Matsumura, 2019) (Gong et al., 2016), and pyrolysis (Gurevich Messina et al., 2017) (Yu et al., 2016).

* Corresponding author at: Jl. Brigjen H. Hasan Basri, Kayu Tangi, Kotak Pos 219, Banjarmasin, Indonesia.
E-mail address: apip.amrullah@ulm.ac.id (A. Amrullah).

https://doi.org/10.1016/j.biteb.2021.100642
Received 31 December 2020; Received in revised form 26 January 2021; Accepted 27 January 2021
Available online 9 February 2021

Pyrolysis is considered the most common method for the thermal conversion of biomass to valuable hydrocarbons and alternative fuels since it is efficient and economical (Gurevich Messina et al., 2017). The products of bio-oils, biogas, and coal can be generated through pyrolysis at 300–600 °C under an inert atmosphere. There have been several attempts to produce bio-oil for fuel as well as high-value chemicals such as phenolic compounds from lignocellulosic biomass using pyrolysis. Naron et al. (2019) studied the phenols production from pyrolysis of hardwood, softwood, and herbaceous lignin under different catalyst agent. The influence of the catalyst was found to differ, depending on the types of lignin. Asadullah et al. (2013) reported that palm residue was an excellent source for phenol production.

Apart from that, several types of biomass such as rice straw (Biswas et al., 2018), waste tire (Seng-eiad and Jitkarnka, 2016), sawdust (Moralı et al., 2016), swine manure (Cheng et al., 2014), algae (Shanmugam et al., 2017), empty fruit bunch (Park et al., 2019), switchgrass (Fortin et al., 2015) have been used to produce bio-oil using pyrolysis. However, there has been no previous study to utilize purun tikus (*Eleocharis dulcis*) as a feedstock of pyrolysis. Therefore, the pyrolysis process of purun tikus (*Eleocharis dulcis*) was studied herein for the first time. Purun tikus (commonly known in Indonesian) is one of the biomasses in the swampland and grows well in acidic water. To the best of the authors' knowledge, this is the first study to investigate the pyrolysis of purun tikus (*Eleocharis dulcis*) leaves and to deduce the detailed reaction kinetics for pyrolysis process. The reaction kinetics is helpful for understanding the reaction behavior. This study aims to evaluate the effect of pyrolysis temperature and particle size on product distributions and bio-oil composition during the pyrolysis of purun tikus (*Eleocharis dulcis*) leaves as well as to deduce the rates of the corresponding reaction.

2. Materials and methods

2.1. Materials

The purun tikus used in this work was collected from the Danau Seran, Banjarbaru, South Kalimantan, Indonesia. Purun tikus was composed of crude protein (8.22%), fiber (25.72%), ether extract (0.48%), ash (15.13%), hemicellulose (19.74%), cellulose (21.80%), and lignin (28.04%) (Muhakka et al., 2020). Meanwhile, the ultimate analysis showed that the purun tikus was composed of N (3.4%), P (0.43%), K (2.0%), Ca (0.3%), Mg (0.4%), S (0.8%), Al (0.6%), and Fe (142.2 mg/l) (Tham , 2012). The plant was washed manually and the leaves were cut and dried in an oven at 105 °C for 24 h before use. After the pulverization process, particle sizes of 20, 40, and 60 μm were achieved. The volatile content was determined using the Thermogravimetric Analyzer (TGA) according to ISO 562:2010. Meanwhile, the ash content was determined using the Muffle furnace (type Furnace Naberthem LE 4/11/R6) according to ASTM D 3174-12, 2009.

2.2. Experimental

The purun tikus was prepared as feedstock and the varied particle sizes of 0.2, 0.4. and 0.6 mm were used. The pyrolysis process was performed in a stainless steel-batch reactor illustrated in Fig. 1. The reactor was equipped with a heater, condenser, and temperature controller. The 220 V electric heater was used and controlled with a PCD controller. A K-type thermocouple was used to measure the temperature. The condenser is composed of a copper tube, and cold water was used as the condensate. The reactor was purged with N_2 for approximately 20 min before each experimental trial. The pressure gauge was used to control the N_2 flow. The feedstock was placed in the reactor and kept at a specified temperature for approximately 30 min, and the volatile was released. The experimental temperatures were varied at 300, 400, and 500 °C. Amount of feedstock as much as 250 g were used. Initially, feedstock was placed inside the reactor and was closed with a bolt. During the process, the condensation process occurred; bio-oil was produced and was separated into the oil phase and water phase. After the reactor was cooled down, the char was collected and weighted. At the end of each experiment, the solid mass that remained in the crucible was assumed as the char yield. The gas yield was determined using argon as a tracer from the ideal gas equation. The yield of products was calculated based on the initial mass of feedstock.

2.3. Bio-oil and char characterization

The chemical composition of bio-oil samples was analyzed using a GC–MS (QP-2010), which employed a capillary column coated with whit Rtx-5MS (i.d. 60 m × 0.25 mm and film thickness of 0.25 μm). 1 mL of sample was dissolved in methanol and injected into the column. The temperature program of GC began at 150 °C, first maintaining this temperature for 5 min. The temperature was then inclined to 300 °C. Each compound was then identified using the standard solution. The solid (char) product was observed using a digital microscope CHR (B80GHM) equipped with 8 LEDs. In this study, the focal length (3–60 mm) and image resolution (640 x 480P) were used. All experimental runs have been carried out in duplicate.

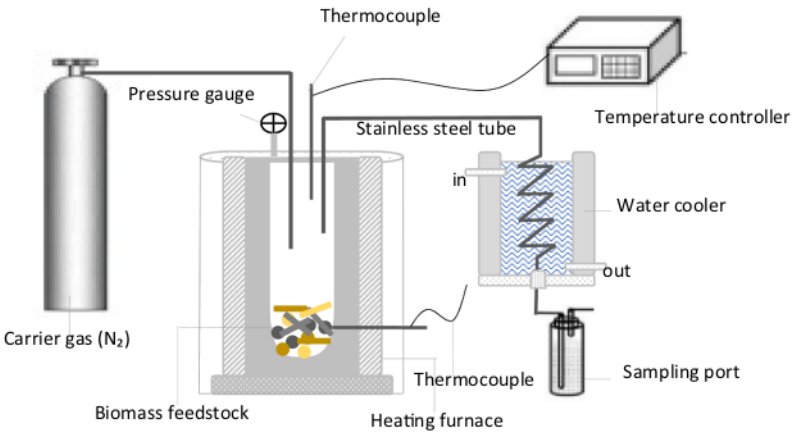

Fig. 1. Experimental apparatus.

3. Results and discussion

3.1. Effect of pyrolysis temperature and particle size on product distribution

The most important operating parameter on the pyrolysis process was the temperature of a chemical process especially those involving the endothermic process. The temperature plays a vital role in providing the heat needed for biomass decomposition. In this study, the temperature was varied at 300, 400, and 500 °C. The bio-oil, bio-char, and gaseous yield were compared as shown in Fig. 2. The combustible gaseous such as H_2 and CO were dominant (38.9% and 31%, respectively), while the hydrocarbons such as CH_4, C_2H_6, and C_3H_6 were merely 18%, 4%, and 1.4%, respectively as the gaseous product. The yield of bio-oil and gaseous is positively affected by changes in temperature. Bio-oil increased from 16 to 31%, followed by an increase in temperature from 300 to 500 °C. Meanwhile, bio-char yield decreased from 62 to 45% by increasing temperature from 300 to 500 °C. These results agreed well with the previous study, which observed that the decrease in the yield of char with the rise in temperature could be attributed to the loss of volatiles, which thermally breaks into low molecular weight organic liquids and gaseous products due to thermal degradation of the lignocellulosic biomass (Chandra and Bhattacharya, 2019; Dhanavath et al., 2019).

The effect of temperature on the morphological structure of purun tikus pyrolysis has been given in Supplementary material. It is clearly shown that temperature has a significant impact on the morphological structure of purun tikus. The solid products displayed an extreme black color with an increase in the temperature of the pyrolysis, along with an increase in the particle size. In terms of the heat transfer during the pyrolysis process, the size of the biomass particles is very influential and contributed to the yield and quality of pyrolysis products (Sirijanusorn et al., 2013). In this work, the small particle size of biomass contributed to the decrease of bio-oil yield (16%); which is correlated with the high bio-char yield (62%). There could be two reasons why the small particle size of biomass gave the lowest bio-oil yield. The first reason is correlated with the high ash content of feedstock because of the segregation of the feed into a high dirt feed. The second explanation is due to the hydrodynamic nature of small particle size of biomass may tend to be entrained out of the reaction zone prior to complete pyrolysis (Pattiya and Suttibak, 2012). Therefore, it is recommended that a small range of biomass particle sizes should be avoided when bio-oil is generated from rapid pyrolysis.

3.2. Effect of temperature on the characteristics of bio-oil

Fig. 3 displays the effect of pyrolysis temperature (300, 400, and 500 °C) on the characteristics of bio-oil with a particle size of 0.6 mm. The figure shows the chromatograms of bio-oil detected by GC–MS from different samples at different temperatures. The general compounds identified by GC–MS were listed in Table 1. The main components were acetic acid, hydroxy acetone, phenol, and furfural. Meanwhile, *o*-cresol, *p*-cresol, guaiacol, methyl propyl ketone, and 2,6 dimethoxyphenol were produced as side products of phenolic compounds. This result trend goes along with Supriyanto et al. (2020) who reported that methoxy groups were performed as the main volatile compound for the fast pyrolysis of alkali lignin. In this work, acetic acid dominated as a compound in the bio-oil product. The yield of acetic acid increased from 31 to 38 (wt%), followed by increasing the temperature; this is most likely indicating that lignin and hemicelluloses were degraded to produce acetic acid

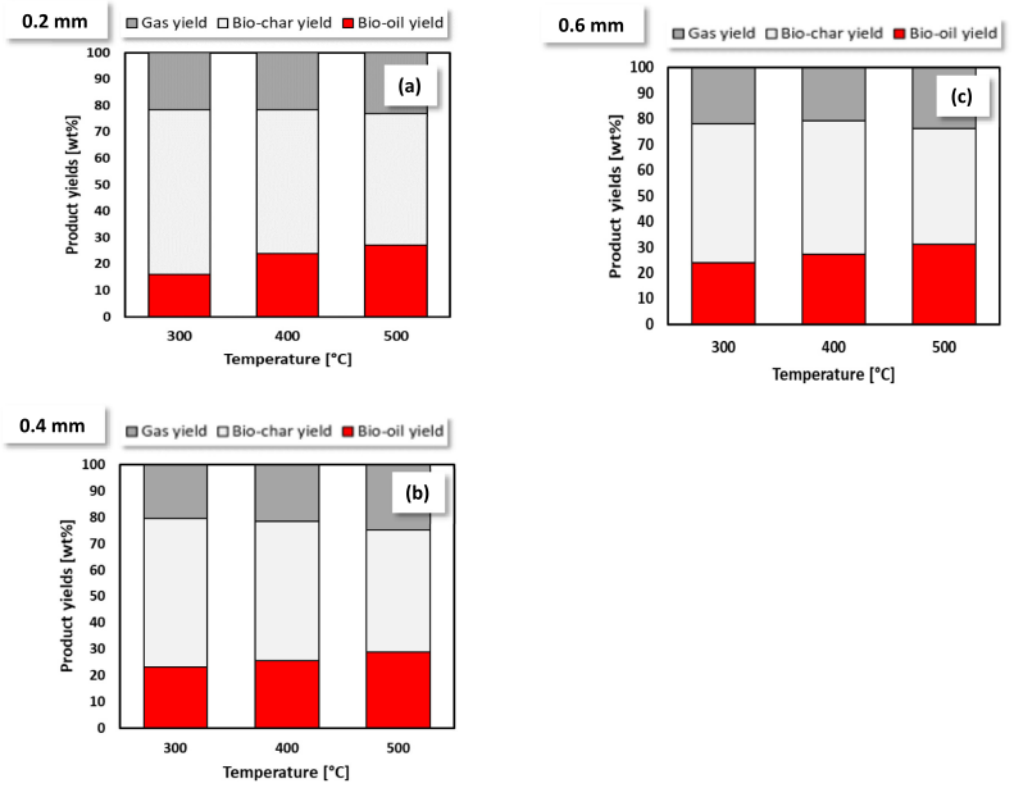

Fig. 2. Effect of temperature and particle size (a) 0.2 mm, (b) 0.4 mm, and (c) 0.6 mm on product distributions of purun tikus pyrolysis.

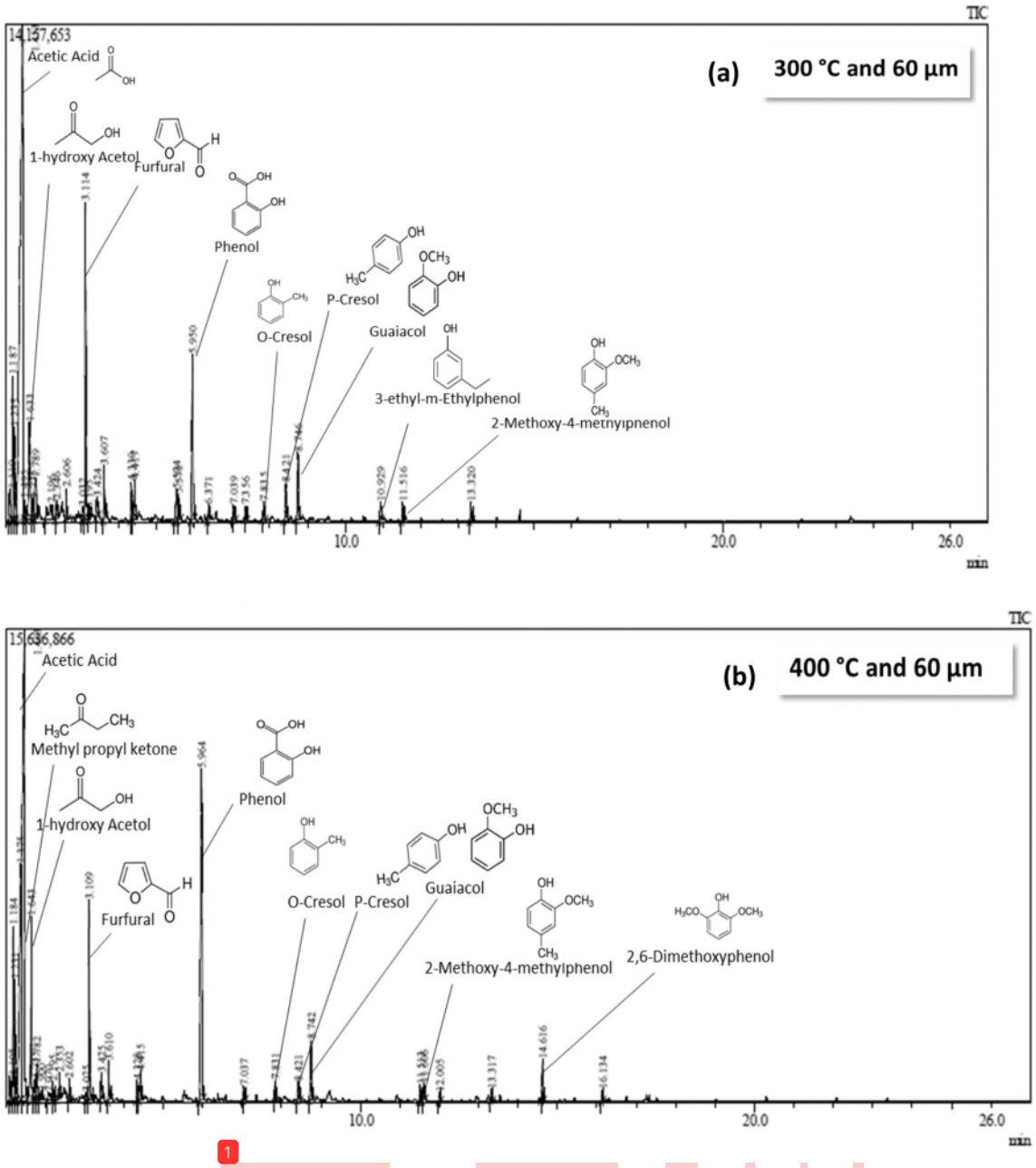

Fig. 3. GC/MS chromatogram of purun tikus bio-oil obtained at (a) 300 °C, (b) 400 °C, and (c) 500 °C.

(Jeffries, 1994; Sjöberg et al., 2004). Not only acid but also phenol can be produced from the degradation of lignin. Zhang et al. (2012) reported that there are two-steps degradation of lignin to produce phenol from pyrolysis of biomass, i.e., firstly, lignin decomposed into different phenolic compounds; secondly, demethylation, decarboxylation, and other phenol reactions were subjected to phenol compounds to generate phenol. In this work, the effect of pyrolysis temperature on phenol production was elucidated. The yield of selective phenol increased by increasing pyrolysis temperature. The maximum phenol content as high as 18.23 wt% was achieved at a maximum temperature of 500 °C. This content is slightly higher than the previous study by Guzelciftci et al. (2020) who obtained the phenol content of 16 wt% from typical one-stage pyrolysis of wood biomass. This should be due to the different lignin content of biomass since phenolic compounds are mainly derived from the degradation of lignin.

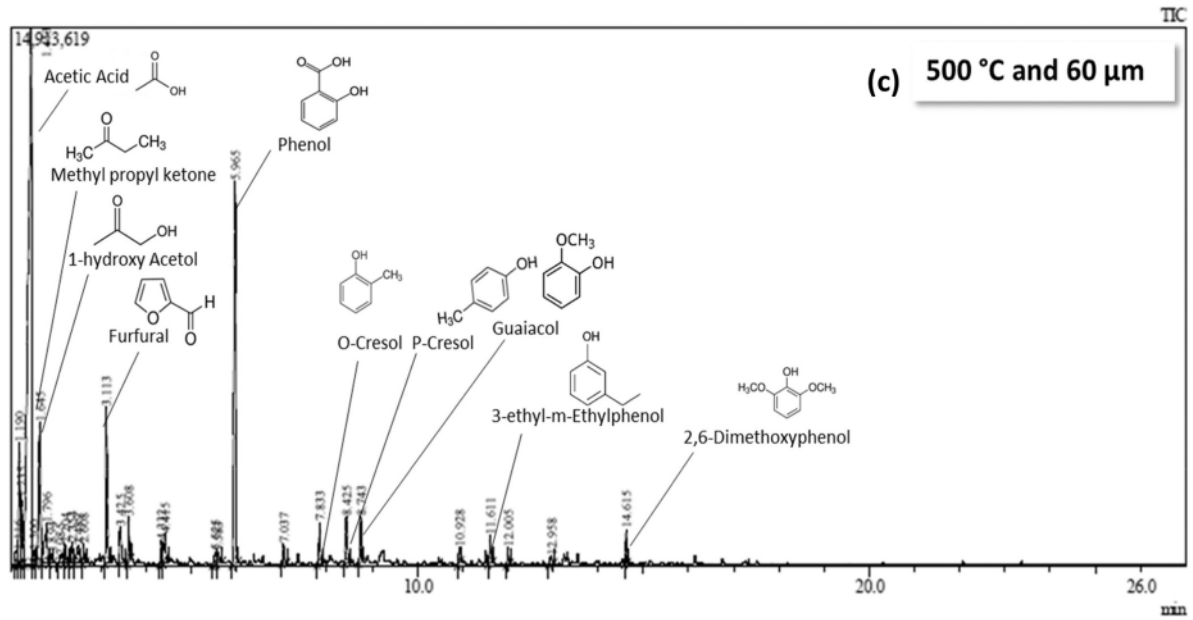

Fig. 3. (*continued*).

Table 1
Compounds identified in purun tikus bio-oil by GC/MS.

No	Compounds name	Formula	Residence time	Percentage under different pyrolysis temperature (%)			Group
				300 °C	400 °C	500 °C	
1	Acetaldehyde	C_2H_4O	1.1	n/a	0.92	n/a	Aldehyde
2	Acetone-oxime	C_3H_7NO	1.18	7.28	4.79	5.34	Ketone
3	Methyl acetate	$C_3H_6O_2$	1.23	6.01	3.46	n/a	Aldehyde
4	Acetic acid	$C_2H_4O_2$	1.45	30.96	31.16	37.53	Acid
5	Tetrahydrofuran	C_4H_8O	1.49	0.51	n/a	0.23	Furfuran
6	Hydroxy acetone	$C_3H_6O_2$	1.63	10.61	5.87	12.95	Alcohol
7	Methyl propyl ketone	$C_5H_{10}O$	1.64	n/a	6.86	n/a	Ketone
8	Propionic acid	$C_3H_6O_2$	1.79	n/a	n/a	1.5	Acid
9	2-Butanone	$C_{18}H_{18}O_3$	1.78	n/a	0.39	n/a	Ketone
10	3-Hydroxy-acetoin	$C_4H_8O_2$	1.89	n/a	0.46	0.61	Ketone
11	Pyrazine	$C_4H_4N_2$	2.07	n/a	0.45	0.31	Aromatic
12	Pyridine	C_5H_5N	2.19	0.83	0.53	0.73	Benzene
13	Diethyl ketone	$C_5H_{10}O$	2.34	1.87	n/a	n/a	Ketone
14	1-Hydroxy-2-butanone	$C_4H_8O_2$	2.35	n/a	1.32	1.44	Ketone
15	Cyclopentanone	C_5H_8O	2.61	1.37	0.62	0.68	Ketone
16	Methylpyrazine	$C_5H_6N_2$	3.03	0.63	0.31	n/a	Ketone
17	Furfural	$C_5H_4O_2$	3.11	10.97	4.21	3.82	Furfuran
18	Isovaleric acid	$C_5H_{10}O_2$	3.19	0.25	n/a	n/a	Acid
19	Furfuryl alcohol	$C_5H_6O_2$	3.42	0.67	0.47	0.76	Alcohol
20	Methyl acetoacetate	$C_5H_8O_3$	3.61	5.02	2.28	3.05	Ketone
21	2-Methyl-2-cyclopentenone	C_6H_8O	4.32	1.12	0.45	0.51	Ketone
22	2-Acetylfuran	$C_6H_6O_2$	4.41	1.75	0.62	0.73	Furfuran
23	5-Methyl-2-furfural	$C_6H_6O_2$	5.52	1.09	n/a	0.31	Furan
24	3-Methyl-2-cyclopentenone	C_6H_8O	5.57	0.65	n/a	0.4	Ketone
25	Phenol	C_6H_6O	5.94	9.5	16.68	18.23	Phenol
26	Cyclohexane	C_6H_{12}	6.37	0.26	n/a	n/a	Alkane
27	2-Cyclopentenone, 2-hydroxy-3-methyl	$C_6H_8O_2$	7.04	0.52	0.35	0.45	Ketone
28	2,3-Dimethyl-2-cyclopentenone	$C_7H_{10}O$	7.35	0.38	n/a	n/a	Ketone
29	Phenol, 2-methyl-*o*-cresol	$CH_3C_6H_4OH$	7.83	0.64	0.48	0.93	Phenol
30	Phenol, 4-methyl-*p*-cresol	C_7H_8O	8.42	1.62	0.67	1.54	Phenol
31	Phenol, 2-methoxy-guaiacol	$C_7H_8O_2$	8.75	2.68	1.81	1.27	Phenol
32	Phenol, 3-ethyl-*m*-ethylphenol	$C_8H_{10}O$	10.93	1.09	n/a	0.64	Phenol
33	2-Methoxy-4-methylphenol	$C_8H_{10}O_2$	11.52	0.59	0.39	n/a	Phenol
34	1,2-Benzenediol-pyrocatechol	$C_6H_6O_2$	11.6	n/a	0.75	1.12	Benzene
35	2-Propenoic acid, 2-methyl-ethyl ester	$C_{11}H_{18}O_4$	12	n/a	0.18	0.3	Acid
36	Phenol, 4-ethyl-2-methoxy-*p*-ethylguaiacol	$C_9H_{12}O_2$	13.32	0.83	0.4	n/a	Phenol
37	2,6-Dimethoxyphenol	$C_8H_{10}O_3$	14.62	n/a	0.94	0.71	Phenol
38	1,2,4-Trimethoxybenzene	$C_9H_{12}O_3$	16.13	n/a	0.24	n/a	Benzene

3.3. Kinetic modeling of purun tikus pyrolysis under different temperature

A detailed kinetics study is needed to examine the characteristics of purun tikus pyrolysis under different operating temperatures. A reaction model was proposed based on the product yields obtained in this study. The solid-phase was directly transformed into the liquid phase (k_{sbo}), while others were converted into the gaseous phase (k_{sg}). In the meantime, the liquid phase could also be decomposed to produce gas (k_{bog}).

The kinetic parameters were calculated by the reaction network to match the experimental data and the model measurement. It is possible to express the change in each product yield as follows:

$$\frac{dY(s)}{dt} = -\left(k_{sbo} + k_{sg}\right)Y(s) \quad (1)$$

$$\frac{dY(bo)}{dt} = k_{sbo}Y(s) - k_{bog}Y(bo) \quad (2)$$

$$\frac{dY(g)}{dt} = k_{sg}Y(s) + k_{bog}Y(bo) \quad (3)$$

where k, t, and $Y(X)$ is reaction rate constant [s^{-1}], reaction time [h], and the yield of product, respectively. The subscript sbo, sg, and bog indicated the reaction direction for solid to bio-oil, solid to gas, and bio-oil to gas, respectively.

Non-linear regression with the least-squares-error (LSE) method (i.e., a common technique in regression analysis to compare experimental and calculation data to find the best fit between them) was used to determine reaction rate constants. Fig. 4 shows the curve fitting between experimental and calculation data. Meanwhile, the reaction rate constants were tabulated in Table 2. For each product yield, the parity plot is shown in Fig. 5(a). There is a strong agreement between the calculation and the experimental data.

To determine the activation energy and pre-exponential factor, the Arrhenius equation (Eq. (4)) was employed.

$$k = Ae^{\frac{-Ea}{(RT)}} \quad (4)$$

where A (pre-exponential factor, [s^{-1}]), Ea (activation energy, [kJ mol^{-1}]), T (reaction temperature [K]), R (constant of universal gas, [8.314 J/mol K]). As illustrated in Fig. 5(b), a straight line was observed between the rate constant (ln$k$) logarithm and the temperature inverse (1/T) logarithm from which the activation energy and pre-exponential factor could be calculated. The activation energies and pre-exponential factors are also presented in Table 2. The activation energy values between 12.65 and 39.18 kJ mol^{-1} were determined for purun tikus pyrolysis. The activation energy values obtained in this study was lower than those of previous works using greenhouse waste (67 to 74 kJ mol^{-1}), algal and lignocellulosic biomass (125 and 113 kJ mol^{-1}), corn stalk (147 to 473 kJ mol^{-1}), and miscanthus (129 to 156 kJ mol^{-1}) (Cortés and Bridgwater, 2015; Leng et al., 2020; Merdun and Laougé, 2021; Vasudev et al., 2019). It is probably due to the chemical composition of each feedstock.

4. Conclusion

Purun tikus was used as a feedstock for pyrolysis to produce bio-oil, bio-char, dan gaseous for the first time. The bio-oil yield (31%) was obtained at 500 °C and 0.6 mm of particle size. The bio-oil yield was affected by particle size distribution. The bio-oil product was mainly composed of acetic acid, hydroxy acetone, phenol, and furfural. The

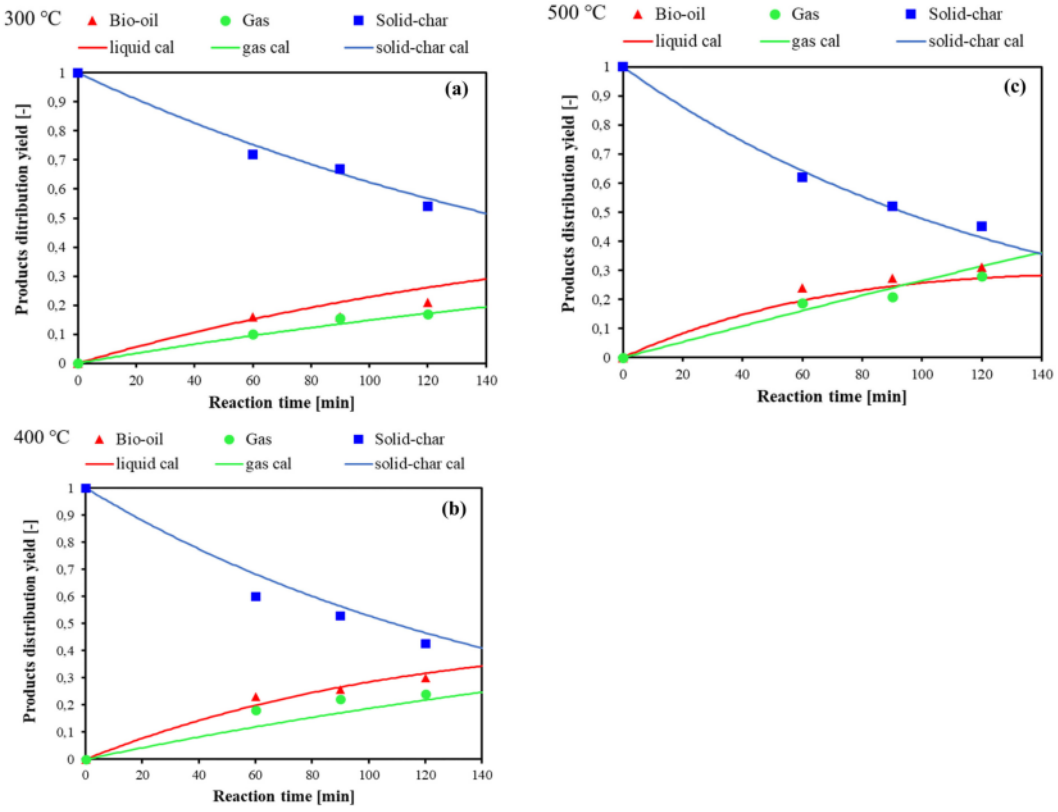

Fig. 4. Effect of reaction temperature and reaction time on the behavior of purun tikus pyrolysis at (a) 300 °C, (b) 400 °C, and (c) 500 °C.

Table 2
Kinetic parameters, activation energies (E_a), and pre-exponential factor (A) (experimental condition: 300–500 °C).

Kinetic Parameter	Reaction direction	Reaction rate constant [s^{-1}] 300 °C	400 °C	500 °C	Activation energy, E_a [kJ mol^{-1}]	Pre-exponential factor, A [s^{-1}]
k_{sbo}	Solid → bio-oil	0.0029	0.0042	0.0047	12.646	0.251
k_{bog}	Bio-oil → gas	0.0018	0.0022	0.0027	15.267	0.477
k_{sg}	Solid → gas	0.0006	0.0047	0.0047	39.178	0.032

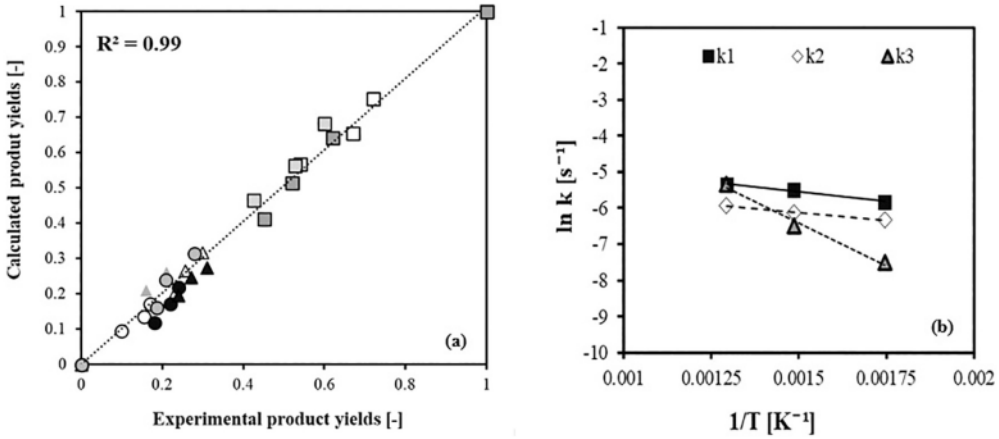

Fig. 5. (a). Comparison of experimental and calculated data of products yield of purun tikus pyrolysis, (b) Arrhenius plot of purun tikus pyrolysis (exp. conditions: 300–500 °C).

highest bio-char yield of 62% was obtained at 300 °C. The kinetic model developed was found to fit well with the experimental results. The activation energies were determined between 12.65 and 39.18 kJ mol^{-1}.

Supplementary data to this article can be found online at https://doi.org/10.1016/j.biteb.2021.100642.

CRediT authorship contribution statement

Apip Amrullah: conceptualization, writing-original draft, methodology, validation, formal analysis, reaction kinetics determination, supervision. **Obie Farobie**: writing-review and editing, validation and data curation, conceptualization, supervision. **Rahmat Widyanto**: conducting experiment, investigation, and analysis.

Declaration of competing interest

The authors declare that they have no known competing financial interests or personal relationships that could have appeared to influence the work reported in this paper.

Acknowledgments

The present study was supported by Lambung Mangkurat University, South Kalimantan, Indonesia

References

Abdeshahian, P., Dashti, M.G., Kalil, M.S., Yusoff, W.M.W., 2010. Production of biofuel using biomass as a sustainable biological resource. Biotechnology 9, 274–282. https://doi.org/10.3923/biotech.2010.274.282.

Amrullah, A., Matsumura, Y., 2019. Sewage sludge gasification under a hydrothermal condition: phosphorus behavior and its kinetics. Energy and Fuels 33, 2301–2307. https://doi.org/10.1021/acs.energyfuels.8b04289.

Asadullah, M., Ab Rasid, N.S., Kadir, S.A.S.A., Azdarpour, A., 2013. Production and detailed characterization of bio-oil from fast pyrolysis of palm kernel shell. Biomass Bioenergy 59, 316–324. https://doi.org/10.1016/j.biombioe.2013.08.037.

Biswas, B., Singh, Rawel, Kumar, J., Singh, Raghuvir, Gupta, P., Krishna, B.B., Bhaskar, T., 2018. Pyrolysis behavior of rice straw under carbon dioxide for production of bio-oil. Renew. Energy 129, 686–694. https://doi.org/10.1016/j.renene.2017.04.048.

Chandra, S., Bhattacharya, J., 2019. Influence of temperature and duration of pyrolysis on the property heterogeneity of rice straw biochar and optimization of pyrolysis conditions for its application in soils. J. Clean. Prod. 215, 1123–1139. https://doi.org/10.1016/j.jclepro.2019.01.079.

Cheng, D., Wang, L., Shahbazi, A., Xiu, S., Zhang, B., 2014. Characterization of the physical and chemical properties of the distillate fractions of crude bio-oil produced by the glycerol-assisted liquefaction of swine manure. Fuel 130, 251–256. https://doi.org/10.1016/j.fuel.2014.04.022.

Cheng, S., Shu, J., Xia, H., Wang, S., Zhang, L., Peng, J., Li, C., Jiang, X., Zhang, Q., 2019. Pyrolysis of Crofton weed for the production of aldehyde rich bio-oil and combustible matter rich bio-gas. Appl. Therm. Eng. 148, 1164–1170. https://doi.org/10.1016/j.applthermaleng.2018.12.009.

Cortés, A.M., Bridgwater, A.V., 2015. Kinetic study of the pyrolysis of miscanthus and its acid hydrolysis residue by thermogravimetric analysis. Fuel Process. Technol. 138, 184–193. https://doi.org/10.1016/j.fuproc.2015.05.013.

Dhanavath, K.N., Bankupalli, S., Sugali, C.S., Perupogu, V., V Nandury, S., Bhargava, S., Parthasarathy, R., 2019. Optimization of process parameters for slow pyrolysis of neem press seed cake for liquid and char production. J Environ Chem Eng 7, 102905. https://doi.org/10.1016/j.jece.2019.102905.

Dhyani, V., Bhaskar, T., 2018. A comprehensive review on the pyrolysis of lignocellulosic biomass. Renew. Energy 129, 695–716. https://doi.org/10.1016/j.renene.2017.04.035.

Fortin, M., Mohadjer Beromi, M., Lai, A., Tarves, P.C., Mullen, C.A., Boateng, A.A., West, N.M., 2015. Structural analysis of pyrolytic lignins isolated from switchgrass fast-pyrolysis oil. Energy and Fuels 29, 8017–8026. https://doi.org/10.1021/acs.energyfuels.5b01726.

Gong, M., Zhu, W., Fan, Y., Zhang, H., Su, Y., 2016. Influence of the reactant carbon-hydrogen-oxygen composition on the key products of the direct gasification of dewatered sewage sludge in supercritical water. Bioresour. Technol. https://doi.org/10.1016/j.biortech.2016.02.070.

Gurevich Messina, L.I., Bonelli, P.R., Cukierman, A.L., 2017. Effect of acid pretreatment and process temperature on characteristics and yields of pyrolysis products of peanut shells. Renew. Energy 114, 697–707. https://doi.org/10.1016/j.renene.2017.07.065.

Guzelciftci, B., Park, K.B., Kim, J.S., 2020. Production of phenol-rich bio-oil via a two-stage pyrolysis of wood. Energy 200, 117536. https://doi.org/10.1016/j.energy.2020.117536.

Jeffries, T.W., 1994. Biochemistry of microbial degradation; 8. Biodegradation of lignin and hemicelluloses. Ratledge C Biochem Microb Degrad 233–277.

Leng, E., Ferreiro, A.I., Liu, T., Gong, X., Costa, M., Li, X., Xu, M., 2020. Experimental and kinetic modelling investigation on the effects of crystallinity on cellulose pyrolysis. J. Anal. Appl. Pyrolysis 152. https://doi.org/10.1016/j.jaap.2020.104863.

Merdun, H., Laougé, Z.B., 2021. Kinetic and thermodynamic analyses during co-pyrolysis of greenhouse wastes and coal by TGA. Renew. Energy 163, 453–464. https://doi.org/10.1016/j.renene.2020.08.120.

Moralı, U., Yavuzel, N., Şensöz, S., 2016. Pyrolysis of hornbeam (Carpinus betulus L.) sawdust: characterization of bio-oil and bio-char. Bioresour. Technol. 221, 682–685. https://doi.org/10.1016/j.biortech.2016.09.081.

Mortensen, P.M., Grunwaldt, J.D., Jensen, P.A., Knudsen, K.G., Jensen, A.D., 2011. A review of catalytic upgrading of bio-oil to engine fuels. Appl. Catal. A Gen. 407, 1–19. https://doi.org/10.1016/j.apcata.2011.08.046.

Muhakka, Suwignyo, R.A., Budianta, D., Yakup, 2020. Nutritional values of swamp grasses as feed for pampangan buffaloes in South Sumatra, Indonesia. Biodiversitas 21, 953–961. doi:10.13057/biodiv/d210314.

Naron, D.R., Collard, F.X., Tyhoda, L., Görgens, J.F., 2019. Influence of impregnated catalyst on the phenols production from pyrolysis of hardwood, softwood, and herbaceous lignins. Ind. Crop. Prod. 131, 348–356. https://doi.org/10.1016/j.indcrop.2019.02.001.

Paksung, N., Matsumura, Y., 2015. Decomposition of xylose in sub- and supercritical water. Ind. Eng. Chem. Res. 54, 7604–7613. https://doi.org/10.1021/acs.iecr.5b01623.

Park, J.W., Heo, J., Ly, H.V., Kim, J., Lim, H., Kim, S.S., 2019. Fast pyrolysis of acid-washed oil palm empty fruit bunch for bio-oil production in a bubbling fluidized-bed reactor. Energy 179, 517–527. https://doi.org/10.1016/j.energy.2019.04.211.

Pattiya, A., Suttibak, S., 2012. Production of bio-oil via fast pyrolysis of agricultural residues from cassava plantations in a fluidised-bed reactor with a hot vapour filtration unit. J. Anal. Appl. Pyrolysis 95, 227–235. https://doi.org/10.1016/j.jaap.2012.02.010.

Rony, A.H., Kong, L., Lu, W., Dejam, M., Adidharma, H., Gasem, K.A.M., Zheng, Y., Norton, U., Fan, M., 2019. Kinetics, thermodynamics, and physical characterization of corn stover (Zea mays) for solar biomass pyrolysis potential analysis. Bioresour. Technol. 284, 466–473. https://doi.org/10.1016/j.biortech.2019.03.049.

Seng-eiad, S., Jitkarnka, S., 2016. Untreated and HNO3-treated pyrolysis char as catalysts for pyrolysis of waste tire: in-depth analysis of tire-derived products and char characterization. J. Anal. Appl. Pyrolysis 122, 151–159. https://doi.org/10.1016/j.jaap.2016.10.004.

Shanmugam, S.R., Adhikari, S., Shakya, R., 2017. Nutrient removal and energy production from aqueous phase of bio-oil generated via hydrothermal liquefaction of algae. Bioresour. Technol. 230, 43–48. https://doi.org/10.1016/j.biortech.2017.01.031.

Sirijanusorn, S., Sriprateep, K., Pattiya, A., 2013. Pyrolysis of cassava rhizome in a counter-rotating twin screw reactor unit. Bioresour. Technol. 139, 343–348. https://doi.org/10.1016/j.biortech.2013.04.024.

Sjöberg, G., Nilsson, S.I., Persson, T., Karlsson, P., 2004. Degradation of hemicellulose, cellulose and lignin in decomposing spruce needle litter in relation to N. Soil Biol. Biochem. 36, 1761–1768. https://doi.org/10.1016/j.soilbio.2004.03.010.

Supriyanto, Usino, D.O., Ylitervo, P., Dou, J., Sipponen, M.H., Richards, T., 2020. Identifying the primary reactions and products of fast pyrolysis of alkali lignin. J. Anal. Appl. Pyrolysis 151. https://doi.org/10.1016/j.jaap.2020.104917.

Thamrin, S.A.M., 2012. Manfaat purun tikus (31), 35–42.

Vasudev, V., Ku, X., Lin, J., 2019. Kinetic study and pyrolysis characteristics of algal and lignocellulosic biomasses. Bioresour. Technol. 288, 121496. https://doi.org/10.1016/j.biortech.2019.121496.

Yu, Y., Chua, Y.W., Wu, H., 2016. Characterization of pyrolytic sugars in bio-oil produced from biomass fast pyrolysis. Energy and Fuels 30, 4145–4149. https://doi.org/10.1021/acs.energyfuels.6b00464.

Zhang, M., Resende, F.L.P., Moutsoglou, A., Raynie, D.E., 2012. Pyrolysis of lignin extracted from prairie cordgrass, aspen, and Kraft lignin by Py-GC/MS and TGA/FTIR. J. Anal. Appl. Pyrolysis 98, 65–71. https://doi.org/10.1016/j.jaap.2012.05.009.

Pyrolysis of purun tikus (Eleocharis dulcis): Product distributions and reaction kinetics

ORIGINALITY REPORT

16%	12%	12%	16%
SIMILARITY INDEX	INTERNET SOURCES	PUBLICATIONS	STUDENT PAPERS

PRIMARY SOURCES

1	Submitted to Institut Pertanian Bogor Student Paper	12%
2	pubag.nal.usda.gov Internet Source	2%
3	Apip Amrullah, Obie Farobie, Gatut Pujo Pramono. "Solid degradation and its kinetics on phenol-rich bio-oil production from pyrolysis of coconut shell and Lamtoro wood residue", Korean Journal of Chemical Engineering, 2022 Publication	2%

Exclude quotes	On	Exclude matches	< 2%
Exclude bibliography	On		